Journal of Power Sources 205 (2012) 301–306

Contents lists available at SciVerse ScienceDirect

Journal of Power Sources

journal homepage: www.elsevier.com/locate/jpowsour

Chromate formation at the interface between a solid oxide fuel cell sealing glass and interconnect alloy

Teng Zhang[a,*], Richard K. Brow[b,**], William G. Fahrenholtz[b], Signo T. Reis[b]

[a] College of Materials Science and Engineering, Fuzhou University, Fuzhou, Fujian 350108, China
[b] Department of Materials Science & Engineering, Missouri University of Science and Technology, Rolla, MO 65409, USA

ARTICLE INFO

Article history:
Received 4 November 2011
Accepted 2 January 2012
Available online 21 January 2012

Keywords:
Solid oxide fuel cells
Sealing glass
Chromate formation
Thermochemical calculation

ABSTRACT

High-temperature interactions between glass–ceramic sealants and Cr-containing ferritic interconnects used in solid oxide fuel cells (SOFC) lead to the formation of detrimental chromate interfacial phases, such as $BaCrO_4$ or $SrCrO_4$, which can cause mechanical failure of the SOFC. In this work, these interactions are characterized by reacting Cr_2O_3 powders with a SrO-containing sealing glass and by characterizing representative reaction couples between the glass and 430 stainless steel. The extent of chromate formation depends on the reaction time and temperature, and the effect of the partial pressure of oxygen is modeled by thermochemical calculations.

1. Introduction

Solid oxide fuel cells (SOFC) have attracted much attention over the last two decades because of their high electrical conversion efficiency, environmental compatibility, and system flexibility [1]. With the reduction of SOFC operational temperatures to under 800 °C, ferritic stainless steels have become favored materials for interconnect components due to their low cost and their close thermal expansion match to other SOFC components [2]. Among the ferritic compositions, chromium-containing alloys attract the most attention due to the high electrical conductivity of the Cr-oxide scale formed on the surface of the alloy during SOFC operation [3].

Interactions between glass–ceramic sealants and ferritic interconnects at the SOFC operational temperatures have been found to result in the formation of interfacial phases potentially detrimental to the performance of the SOFC stacks [4–8]. Alkali ions or residual water in some glass compositions significantly increase the vaporization of chromium from the interconnects [4,11]. Subsequent deposition of the chromium compounds on the cathode blocks the active sites needed for efficient operation. In addition, the transport of Cr-vapors, as CrO_3 or $CrO_2(OH)_2$, can lead to the formation of alkaline earth chromates on glass surfaces well-removed from the glass–metal interface [11]. The high coefficients of thermal expansion (CTE) of these chromates, e.g., $BaCrO_4$ and $SrCrO_4$ ($\sim$18–20 $\times 10^{-6}\,K^{-1}$) [9], contributes to the physical separation of the sealing glass (CTE $\sim 12.5 \times 10^{-6}\,K^{-1}$) and the interconnect ($\sim 13 \times 10^{-6}\,K^{-1}$) because of the large CTE differences, and leads to significant losses in bond strength between SOFC glasses and interconnect materials [10].

The extent and nature of the reactions between glass sealants and different types of alloys depend on the alloy compositions and the exposure conditions [5,11]. For chromia-forming alloys, the edges of the seals where oxygen or air is accessible typically exhibit $BaCrO_4$ formation. For a more oxidation resistant alloy, e.g., a Ni-based superalloy, the extent of the formation of $BaCrO_4$ can be limited. The addition of aluminum to the interconnect alloy can suppress the formation of interfacial chromates and so lead to stronger glass–metal seals [12]. Likewise, the addition of protective coatings to the interconnects has been used to suppress chromate formation [13], but often at the cost of conductivity.

Therefore, the information on the interfacial reactions between sealing glass and Cr-containing interconnect alloys is critical for the performance of SOFC stacks. However, there are few reports on the comprehensive characterization of such reactions in literature, especially for the quantitative analysis due to the complex structure of sealing couples [14,15].

In the present paper, a SrO-containing sealing glass was reacted with Cr_2O_3 powder to simulate the interfacial reactions between glasses and Cr-containing interconnect alloys during sealing and under subsequent operational conditions. Previous results show that this glass has a CTE of about $12.5 \times 10^{-6}\,K^{-1}$ after sealing process (e.g., 850 °C for 2 h) and maintains substantial amount of residual glass after the crystallization at 800 °C for one month, which provides desired viscous flow for releasing stress in SOFC fixture [16,17]. The formation of $SrCrO_4$ was characterized by optical

* Corresponding author. Tel.: +86 591 22866540; fax: +86 591 22866537.
** Corresponding author. Tel.: +1 573 341 6812; fax: +1 573 341 6934.
E-mail addresses: teng_zhang@fzu.edu.cn (T. Zhang), brow@mst.edu (R.K. Brow).

0378-7753/$ – see front matter © 2012 Elsevier B.V. All rights reserved.
doi:10.1016/j.jpowsour.2012.01.043

Table 1
Composition of glasses (in mole %).

Glass ID	SrO	CaO	B_2O_3	Al_2O_3	SiO_2	TiO_2
G36	26.48	26.48	1.92	1.96	41.16	2.00

spectroscopy, and modeled by thermochemical calculations. These results are compared to those obtained by analyzing the interfaces between the sealing glass and 430 stainless steel (430SS) samples, using scanning electron microscopy (SEM) with energy dispersive analysis by X-ray (EDAX), and the surface of reaction couples by Auger electron spectroscopy.

2. Experimental

A fifty gram sample of the glass composition designated glass #36 (Table 1) was prepared by melting a homogeneous mixture of reagent grade $SrCO_3$, $CaCO_3$, boric acid, and various oxides in a platinum crucible at 1500 °C for 2 h in air. The melt was quenched on a steel plate to form the glass.

The glass was crushed to form powders with particle sizes between 45 and 53 μm. The glass powders were mixed with 10 wt% chromium oxide (Cr_2O_3, Alfa Aesar, >98% purity) powder (similar particle size) for 24 h in a roller mixer. The amount of Cr_2O_3 powder was chosen to yield a Sr:Cr atomic ratio of ~2.5 in each mixture to ensure that the SrO content in the glass was sufficient to fully react with the Cr_2O_3 available under conditions where the formation of $SrCrO_4$ is favored.

Optical spectroscopy (Cary 5E, Varian, Inc.) was used to analyze solutions prepared by dissolving glass/Cr_2O_3 reaction couples (described below) in water. Calibration solutions were prepared by dissolving K_2CrO_4 (Fisher ACS grade) into deionized water to produce a series of Cr^{6+}-containing solutions (ranging from 2 to 25 ppm).

Mixtures of ~15 mg of glass and 1.5 mg of Cr_2O_3 were heated in an alumina boat in air at temperatures between 800 and 950 °C for up to 24 h. After heating, the mixture was dissolved into ~150 ml of room temperature deionized water and the absorption spectra were recorded using UV–vis spectrometry. The concentration of Cr^{6+} in each solution was calculated by fitting the corresponding absorbance using the calibration curve derived from the K_2CrO_4 solutions. Three samples were made under identical conditions and were analyzed to determine the experimental uncertainty. The total concentrations of Cr ions dissolved in each solution were obtained by ICP-OES, and the percent of chromium present as Cr^{6+} in each sample is reported. Similar reaction samples were analyzed by X-ray diffraction (XDS 2000, Scintag, Inc.).

The G#36 sealing glass was bonded to 430 stainless steel substrates and the interfacial reactions were characterized. Glass pastes were prepared by mixing ~50 mg glass powder (45–53 μm) with ~50 μl acetone. The pastes were applied to the ultrasonically cleaned (in the deionized water) surfaces of 430SS substrates; a typical coating was 200 μm thick after sintering. The coated samples were then heated in air from room temperature to the predetermined sealing temperature (e.g., 900 °C) at a heating rate of 10 °C min^{-1}, and held for 2 h. Some 'as sealed' samples were subsequently held in air at 800 °C for up to two weeks. Depth profiles of Cr on the surfaces the glass/430SS samples were determined using Auger electron spectroscopy (Model 545, Physical Electronics), with an Ar ion sputter rate of 2 nm min^{-1}.

Some of the sealed samples were cross-sectioned by a diamond saw and polished using SiC paper from 320 to 1200 grit, and then finished using a diamond suspension (3 μm). The polished samples

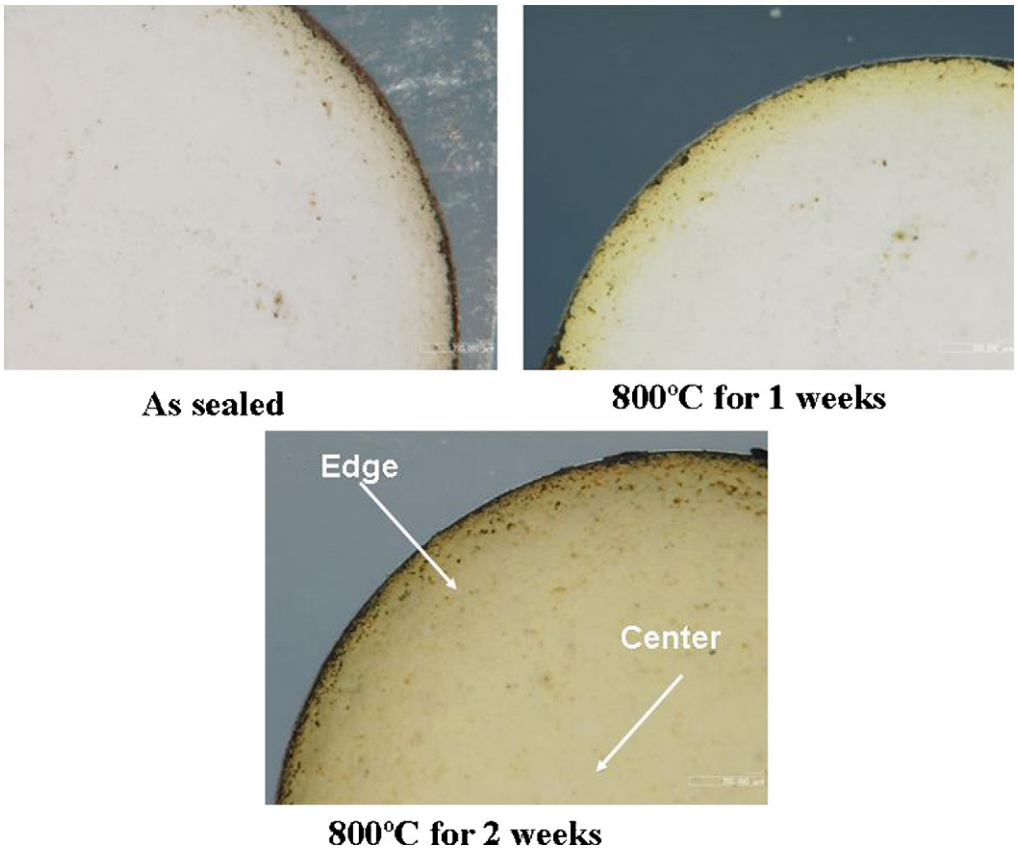

Fig. 1. Optical images of a G#36/430SS couple after heating in air at 800 °C for different times.

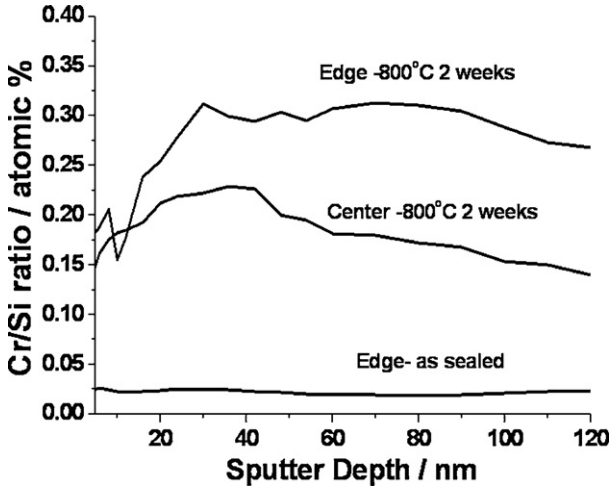

Fig. 2. The AES depth profile on the surface of G#36/430SS seals, 'as sealed' and after the heat treatment in air at 800 °C for 2 weeks.

were analyzed using field emission scanning electron microscopy (S4800, Hitachi, Inc.) and energy dispersive analysis by X-rays (EDAX, Hitachi, Inc.).

3. Results

Fig. 1 shows optical micrographs of the glass-side of a G#36/430SS reaction couple immediately after sealing, and after heating in air for one and two weeks at 800 °C. The yellowish reaction product that can be seen 'growing in' from the edge of the G#36 sample, where the underlying steel is exposed to the air, is an indication of the presence of a chromate phase on the sample surface.

Fig. 2 shows the results of Auger electron spectroscopic depth profiles from two regions of the G#36/430SS reaction couples indicated in Fig. 1. The Cr:Si ratios near the edge and at the center of the sample heated in air for two weeks at 800 °C are significantly greater than that collected from the edge of the 'as sealed' sample.

Fig. 3 shows thin-film XRD data collected from the sample heated in air for two weeks at 800 °C. In addition to the crystalline phases associated with the bulk glass ceramic (Sr_2SiO_4 and $CaSiO_3$), the presence of $SrCrO_4$ is confirmed in this sample.

The reactions that lead to the apparent formation of the yellow chromate phases shown in Fig. 1 were studied by reacting glass samples with Cr_2O_3 powders in air, and the formation of Cr^{6+} in these samples was quantitatively measured using UV–vis spectrometry. Fig. 4 shows absorption spectra collected from solutions of several samples dissolved in water. There are two distinct peaks, centered near 270 and 370 nm, in the spectrum collected from an aqueous solution with 10 ppm Cr^{6+} (from K_2CrO_4) and these are both assigned to Cr^{6+} ions, in agreement with previous studies [18,19]. The extinction coefficient at 370 nm obtained from a series of solutions with Cr^{6+} concentrations from 2.5 to 25 ppm was $4260 \pm 80\ L\,cm^{-1}\,mol^{-1}$, which was close to the value reported for Cr^{6+} in silicate glasses of $4218\ L\,cm^{-1}\,mol^{-1}$ [20].

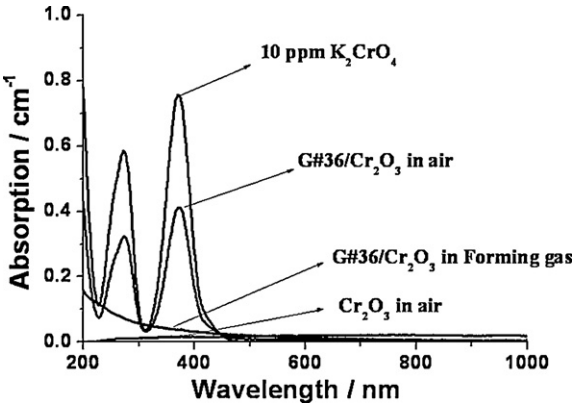

Fig. 4. The absorption spectra of a solution of K_2CrO_4 (10 ppm), and of mixtures of G#36 and 10 wt% Cr_2O_3 held in air and forming gas (10% H_2/90% N_2) at 950 °C for 24 h, then dissolved in water. A solution of Cr_2O_3 held in air at 950 °C for 24 h, then dissolved in water, is also shown.

Also shown in Fig. 4 are absorption spectra of solutions prepared from the dissolved mixtures of glass #36 and Cr_2O_3 heated to 950 °C for 24 h in air and heated to 950 °C for 24 h in a reducing atmosphere (10% H_2/90% N_2). The absorption spectrum of pure Cr_2O_3 powder treated in air is also included for comparison. For the glass/Cr_2O_3 mixture heated in air, the spectrum reveals peaks centered at 270 nm and 370 nm, corresponding to absorption by Cr^{6+} ions. These peaks are not evident for the mixture heated in reducing conditions or for the pure Cr_2O_3 heated in air. Using the extinction coefficient determined from the calibration runs, the absorbance at 370 nm, and the Cr-content of the solution obtained by ICP, one calculates that about 68% of the total chromium in the Glass#36/Cr_2O_3 mixture is oxidized to form a chromate after 24 h in air at 950 °C.

Fig. 5 shows the percentage of Cr^{6+} formed from Cr_2O_3 mixtures with G#36 after heating in air to temperatures ranging from 800 °C to 950 °C for up to 24 h. The percentage of Cr^{6+} increased with

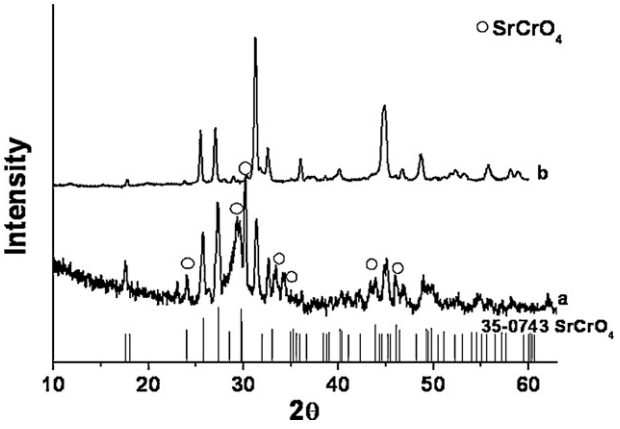

Fig. 3. Thin film XRD pattern (a) for the yellowish product at the interface between G#36 and 430SS after heating in air at 800 °C for 2 weeks, and the XRD pattern (b) G#36 alone after heating in air at 950 °C for 24 h.

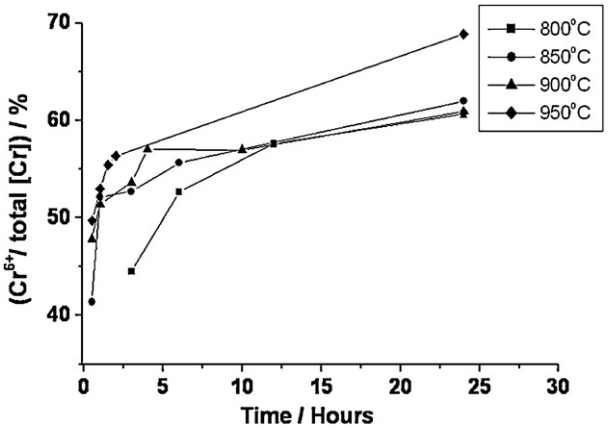

Fig. 5. The fraction of Cr^{6+} in the reaction couples between Cr_2O_3 and G#36 as a function of time in air at different temperatures. The error bar indicates experimental uncertainty. The solid lines are guides for the eye.

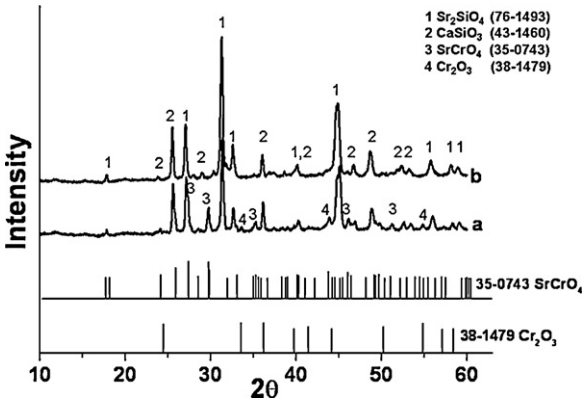

Fig. 6. XRD patterns from (a) the G#36/Cr_2O_3 reaction couple and (b) G#36 alone after heating in air at 950 °C for 24 h.

increasing time and temperature, although the time dependence fits no specific kinetic reaction model.

The XRD patterns for G#36 mixed with 10 wt% Cr_2O_3 heat-treated in air at 950 °C for 24 h reveals the presence of $SrCrO_4$ and some residual Cr_2O_3 [21], as shown in Fig. 6. The XRD pattern for G#36 with no Cr_2O_3 after the same heat treatment is also included for comparison. Both patterns show the presence of Sr_2SiO_4 and $CaSiO_3$, the dominant phases in these glass–ceramics.

4. Discussion

The double-layer oxide scale structure ($(Mn, Cr)_3O_4$ spinel on top of Cr_2O_3) is usually formed on ferritic stainless steels [22]; however, there is only Cr_2O_3 in the oxide scale of 430SS with the presence of Mn–Co protection coating [23]. It is similar to the condition of present work, in which the Mn–Cr spinel phase cannot be formed with the cover of glass coating, and therefore Cr mainly origins from the Cr_2O_3 oxide layer. Sr-chromate ($SrCrO_4$) forms when SrO-containing glasses react with both Cr_2O_3 powders and with 430SS substrates when heated in air to at least 800 °C. One possible path for the formation of $SrCrO_4$ is described by reaction (1):

$$SrO_{(glass)} + 1/2Cr_2O_{3(solid)} + 3/4O_2 \leftrightarrow SrCrO_{4(solid)} \quad (1)$$

Fig. 4 shows that when Cr_2O_3 reacts with a SrO-containing glass, the percentage of Cr^{6+} increases as the heat-treatment time increases for temperatures ranging from 800 °C to 950 °C, and the percentage of Cr^{6+} generally increases with an increase in temperature. The maximum percentage of Cr^{6+} observed was around 70% for the sample heated for 24 h at 950 °C, the highest temperature in this work. The XRD results (Fig. 6) reveal the presence of residual Cr_2O_3 in this same sample, indicating that the reaction to form $SrCrO_4$ may have reached an equilibrium under these conditions, despite the presence of excess SrO in the glass.

Fig. 7a shows the free energy of formation for $SrCrO_4$, from reaction (1), as a function of temperature, and Fig. 7b shows the free energy of formation at 900 °C as a function of the partial pressure of oxygen. These calculations were done using standard free energies reported in Ref. [24]. Fig. 7a indicates that reaction (1) is favored at all temperatures for an oxygen partial pressure of 0.2 atm. However, Fig. 7b indicates that the free energy of the formation of $SrCrO_4$ decreases with decreasing oxygen partial pressure, and becomes positive at 900 °C for partial pressures less than $10^{-7.2}$ atm. For example in air, the formation of $SrCrO_4$ is thermodynamically favored 900 °C (free energy is −158 kJ mole^{-1} at 0.2 atm), but it is not favored under forming gas (+213 kJ mole^{-1} at 10^{-16} atm). These calculations are consistent with the analyses of Cr^{6+} ions from Cr_2O_3/glass reaction couples (i.e., Fig. 4) and from observations of glass/430SS seals heated in air and in reducing conditions, and are similar to the reports of chromate formation with BaO- and SrO-containing glasses [5–7].

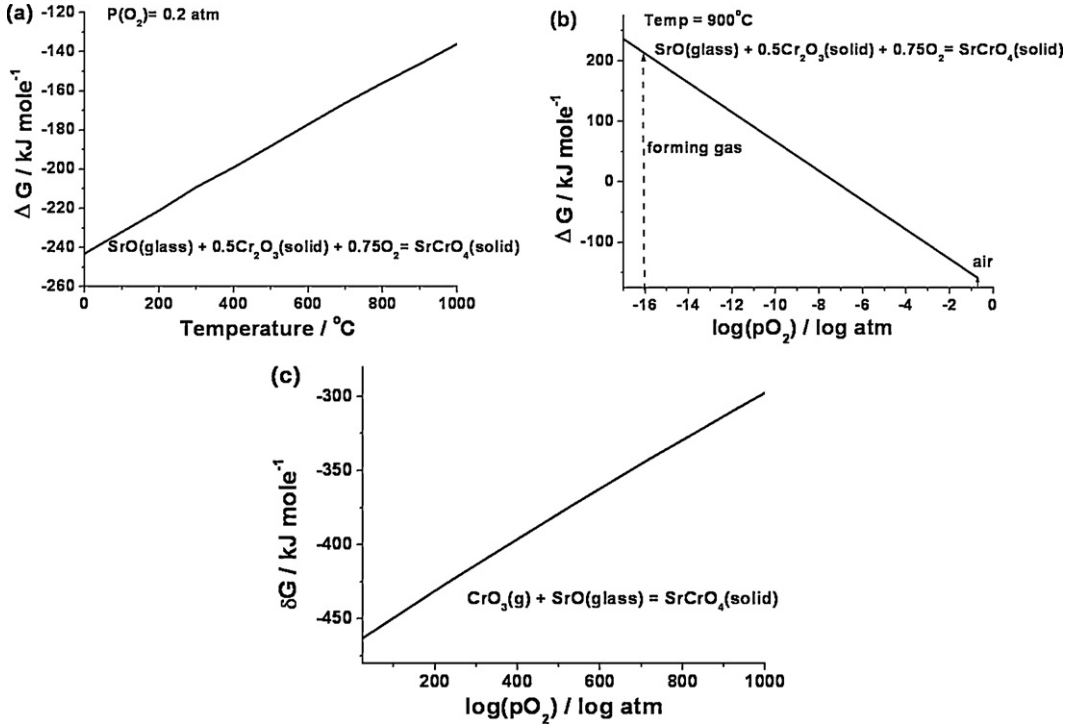

Fig. 7. (a) Gibbs free energy for reaction (1) as a function of temperature, (b) Gibbs free energy of the formation of $SrCrO_4$ (reaction (1)) at 900 °C as a function of the partial pressure of oxygen and (c) Gibbs free energy for reaction (3) as a function of temperature.

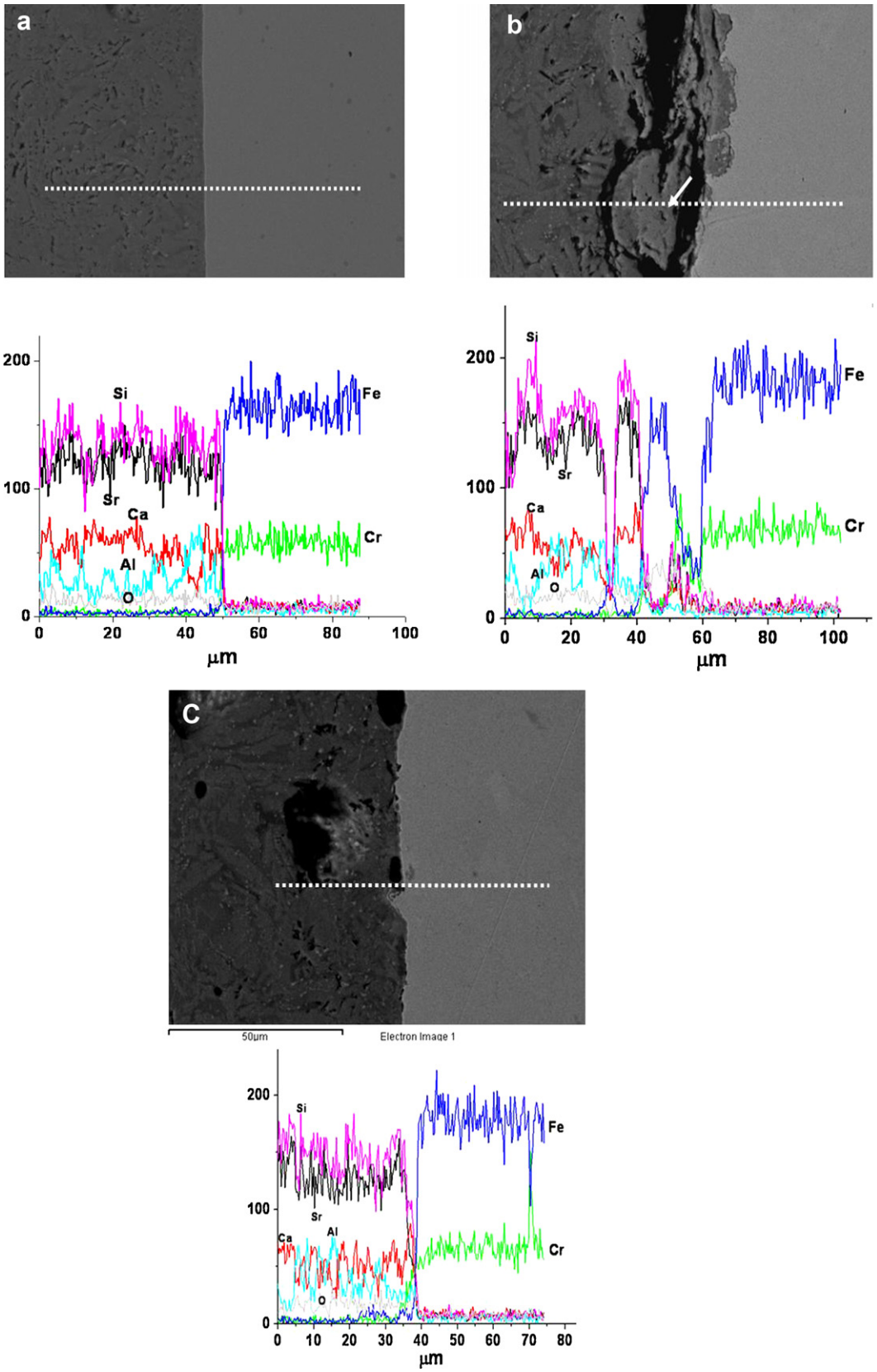

Fig. 8. SEM images and EDS line scans for the interfaces of G#36/430SS, (a) as sealed, edge, (b) after heating in air at 800 °C for 2 weeks, edge and (c) after heating in air at 800 °C for 2 weeks, center. The line scans were collected along the dashed line indicated in each micrograph.

A second possible path involves the interaction between SrO in the glass and Cr-vapors from thermodynamically unstable chromia scales [25]:

$$Cr_2O_{3(solid)} + 1.5O_{2(g)} \leftrightarrow 2CrO_{3(g)} \quad (2)$$

$$CrO_{3(g)} + SrO_{(glass)} \leftrightarrow SrCrO_{4(solid)} \quad (3)$$

Fig. 7c shows that reaction (3) is thermodynamically favored under the conditions of the current experiments, and so this reaction seems the likely source for the spread with time of the yellow chromate phase across the surface of the G#36/430SS reaction couple shown in Fig. 1. A similar vapor transport mechanism was proposed for the formation of $BaCrO_4$ on the surface of a Ba-containing SOFC sealing glass some distance away from the glass–metal interface [11].

Shown in Fig. 8 are micrographs of the interfaces between G#36 and 430SS, 'as sealed' (8a) and after heating in air at 800 °C for 2 weeks (8b). These images were taken near the edges of each sealed sample. Fig. 8c shows a micrograph of the latter sample near the center of the seal, well away from the edge. Also shown are EDS elemental line scans taken across the respective interfaces. For the 'as-sealed' sample, the crystallized glass forms a continuous interface with the 430SS and there is little evidence for either significant interfacial reaction products or the diffusion of metal species into the glass, or vice versa. The interface of the heat-treated sample near the center of the seal (8c) is also continuous, but a bit rougher. There are no obvious second phases, but there is evidence for the diffusion of some Cr about 5–10 μm into the glass. This contrasts with the significant changes after heat-treatment in the interfacial region near the seal edge (Fig. 8b). The glass–ceramic has separated from the metal, the metal interface is much rougher than it is in the 'as sealed' sample or in the heat-treated sample at the center of the seal, oxide components are adhered to, and penetrate into the metal, and a new oxide phase has formed between the glass–ceramic and the metal. The EDS line scan of this sample shows coinciding enrichments of Cr and Sr in certain regions of the new oxide phase, along with enrichments of Fe. The Sr:Cr atomic ratio in the region indicated by the arrow in Fig. 8b is 1.1 ± 0.2. These results are consistent with the formation of $SrCrO_4$ at this interface. These reactions occur near the edge of the seal where oxygen is available to produce $SrCrO_4$ (Eq. (1)). At the seal center (Fig. 8c), there is no pathway available for oxygen, and so this reaction does not occur. Instead, Cr dissolves into the glass to form a Cr-rich interface region that has been noted in other SOFC glass/interconnect systems [8,11]. The Mn content in 430SS is negligible (about 0.5 wt%), and therefore, has not been included in EDS linescan.

5. Conclusions

The formation of $SrCrO_4$ was observed in mixtures of a SrO-containing SOFC sealing glass and Cr_2O_3 powders, and with glass/430SS reaction couples. Cr transports from the 430SS to the glass interface, or the glass surface and in the presence of oxygen reacts to form $SrCrO_4$. Thermochemical calculations reveal that this reaction is thermodynamically favored in air, and this is consistent with the observation of $SrCrO_4$ at interfaces with access to air: at seal edges, not seal centers. In the center of the seal, Cr dissolves into the glass to form a thin (<10 μm) Cr-rich region.

Acknowledgements

The authors gratefully acknowledge the financial support of Department of Energy/SECA (Project NT42221), the National Natural Science Foundation of China (No. 51102045), the Ph.D. Programs Foundation of Ministry of Education of China (No.20103514120006), funds for Distinguished Young Scientists from the Fujian Education Department (No. JA11007) and the funding (type A) (No. JA09020) from the Fujian Education Department of China. They would also like to thank colleagues at Missouri S&T, Eric Bohannan for assistance with X-ray diffraction, Nathan Miller for assistance with ICP-OES, and Jeffry Wight for assistance with the AES, and Fanrong Zeng (Fuzhou University) for assistance with the SEM/EDS analysis.

References

[1] S. Singhal, Am. Ceram. Soc. Bull. 82 (2003) 19–20.
[2] P. Kofstad, R. Bredesen, Solid State Ionics 52 (1992) 69–75.
[3] Z. Yang, K.S. Weil, D.M. Paxton, J.W. Stevenson, J. Electrochem. Soc. 150 (2003) A1188–A1201.
[4] N. Lahl, D. Bahadur, K. Singh, L. Singheiser, K. Hilpert, J. Electrochem. Soc. 149 (2002) A607–A614.
[5] Z. Yang, J.W. Stevenson, K.D. Meinhardt, Solid State Ionics 160 (2003) 213–225.
[6] Z. Yang, G. Xia, K.D. Meinhardt, K.S. Weil, J.W. Stevenson, J. Mater. Eng. Perform. 13 (2004) 327–334.
[7] Y.-S. Chou, J.W. Stevenson, R.N. Gow, J. Power Sources 170 (2007) 395–400.
[8] T. Jin, K. Lu, J. Power Sources 195 (2010) 4853–4864.
[9] J.W. Fergus, J. Power Sources 147 (2005) 46–57.
[10] Y.-S. Chou, J.W. Stevenson, P. Singh, J. Power Sources 184 (2008) 238–244.
[11] Z. Yang, K.D. Meinhardt, J.W. Stevenson, J. Electrochem. Soc. 150 (2003) A1095–A1101.
[12] Y.-S. Chou, J.W. Stevenson, P. Singh, J. Power Sources 185 (2008) 1001–1008.
[13] G. Cabouro, G. Caboche, S. Chevalier, P. Piccardo, J. Power Sources 156 (2006) 39–44.
[14] S.T. Misture, SECA final report, Department of Energy, 2005.
[15] T. Zhang, H. Zhang, G. Li, H. Yung, J. Power Sources 195 (2010) 6795–6797.
[16] T. Zhang, Ph.D Thesis, Ceramic Engineering, Missouri University of Science and Technology, Rolla, 2008.
[17] S.T. Reis, R.K. Brow, J. Mater. Eng. Perform. 15 (2006) 410–413.
[18] T. Murata, M. Torisaka, H. Takebe, K. Morinaga, J. Non-Cryst. Solids 220 (1997) 139–146.
[19] M.M. Sena, I.S. Scarminio, K.E. Collins, C.H. Collins, Talanta 53 (2000) 453–461.
[20] P. Nath, A. Paul, R.W. Douglas, Phys. Chem. Glasses 6 (1965) 203–206.
[21] Joint Committee on Powder Diffraction Standards, International Centre for Diffraction Data, Swarthmore, USA, 2001.
[22] S.P. Simner, M.D. Anderson, G.G. Xia, Z. Yang, L.R. Pederson, J.W. Stevenson, J. Electrochem. Soc. 152 (2005) A740–A745.
[23] B. Hua, J. Pu, W. Gong, J. Zhang, F. Lu, L. Jian, J. Power Sources 185 (2008) 419–422.
[24] M.W. Chase, NIST-JANAF Thermochemical Tables, American Chemical Society, Woodbury, New York, 1998.
[25] Y. Matsuzaki, I. Yasuda, J. Electrochem. Soc. 148 (2001) A126–A131.